# Hopfions in the Lee-Huang-Yang superfluids

# Liangwei Dong\*

Department of Physics, Zhejiang University of Science and Technology, Hangzhou, 310023, China

### Mingjing Fan

The MOE Key Laboratory of Weak-Light Nonlinear Photonics, TEDA Applied Institute and School of Physics, Nankai University, Tianjin, 300457, China

Boris A. Malomed

Department of Physical Electronics, School of Electrical Engineering, Faculty of Engineering, Tel Aviv University, Tianjin, 300437, China

Boris A. Malomed

Department of Physical Electronics, School of Electrical Engineering, Faculty of Engineering, Tel Aviv University, Tel Aviv 69978, Israel

Institute of Alsa Investigacion, Universidad de Tarapaca, Cassilla 7D, Arica, Chile

Yaroslav V, Kartashov

Institute of Spectroscopy, Russian Academy of Sciences, Troitisk, Moscon; 108840, Russia

Abstract

It is known that, under appropriate conditions, mean-field interactions can be canceled in binary BEC, leading to the formation of the Lee-Huang-Yang (LHY) superfluid, in which the nonlinearity is solely represented by the quartic LHY term. In this work we systematically investigate the existence, stability and evolution of hopfion states in this species of quantum matter. They are characterized by two independent topological winding numbers: inner twist s of the wortex-ring core and overall vorticity m. The interplay between the LHY self-repulsion and a trapping harmonic-oscillator potential results in stability of the hopfions whilst distinct topological phase distributions along the vertical axis and the radial direction in the horizontal plane. Their effective radius and peak density increase with the chemical potential, along with expansion of the vortex-ring core, Although the instability domain of the hopfion modes broadens with the increase of m, stable hopfions persist in a wide range of the chemical potential, up to m = 4, at least, provided that the norm exceeds a certain threshold value. The predictions are experimentally accessible in currently used BEC setups.

\*\*Keywords:\*\* Hopfions; Vorticity; Topological charge; Mean-field theory; LHY corrections; Superfluids; Stability.

\*\*Introduction\*\*

1. Introduction\*\*

The creation of stable three-dimensional (3D) nonlinear states is a fundamental challenge across diverse areas of physics, including optics [1, 2], Bose-Einstein condensates (BE

3D hard-sphere gas (i.e., with repulsive interactions between particles) [14]. This correction, known as the Lee-Huang-Yang (LHY) term, quantifies the impact of quantum fluctuations of the dynamics of the atomic BEC [15, 16]. In particular, the correction plays a crucial role in stabilizing ultracold atomic

\*Corresponding author. Email address: dlw0@163.com (Liangwei Dong)

avoid the collapse inherent in pure MF systems. The interplay between contact repulsion and dipole-dipole attraction has led to the observation of anisotropic quantum droplets in dipolar gases [31, 32]. Subsequently, nearly 2D [22, 23] and 3D isotropic QDs [33] have been experimentally realized and theoretically investigated in mixtures of two atomic states in <sup>39</sup>K. Further, QDs have been created in attractive mixtures of <sup>41</sup>K and <sup>87</sup>Rb atoms with contact interactions [34], and in binary dipolar BECs [35, 36]. Self-evaporation dynamics of quantum droplets was investigated in a <sup>41</sup>K and <sup>87</sup>Rb mixture [37].

In addition to QDs stabilized by the interplay of the MF and LHY effects in binary BEC mixtures, Jørgensen et al. have predicted that, in the binary condensates with atom numbers of the two components,  $N_1$  and  $N_2$ , and the intra- and inter-component interaction coefficients,  $g_{11,22}$  and  $g_{12}$ , precisely tuned to specific conditions,  $\sqrt{g_{11}}N_1 = \sqrt{g_{22}}N_2$  and  $g_{12} = -\sqrt{g_{11}g_{22}}$ , the effective MF interactions entirely vanish due to mutual cancellation, leaving the system (LHY superfluid) governed solely by quantum fluctuations [38]. An effective one-component Gross-Pitaevskii equation (GPE) accurately describes the dynamics of the LHY superfluids in this case, as confirmed by the comparison with the full two-component system. Experimentally, such 3D LHY superfluids have been realized in a <sup>39</sup>K spin mixture confined in a spherical trap [39]. Recently, the 1D counterpart of the LHY superfluid has also been studies theoretically [40]. Nevertheless, so far only the simplest states with trivial phases were studied in LHY quantum superfluids. Here we show that, in the presence of an external trapping potential, this state of quantum matter can as well support stable topological modes with a highly nontrivial phase structure called hopfions.

Hopfions are 3D topologically organized states named after Heinz Hopf, who discovered the Hopf fibration in 1931 [41]. These 3D states, which were originally identified in the field theory, exhibit robust particle-like characteristics. Inheriting the topological properties of the Hopf fibration, they are defined by a homotopic mapping from a unit sphere in the 4D space to the 3D unit sphere. Hopfions represent a special class of toroidal modes [42], which are characterized by two independent winding numbers: a hidden twist (*s*), which represents a circular vortex thread, and the overall vorticity around the vertical axis (*m*). Hopfions have been demonstrated in various areas, including the field theory [43, 44], magnetic materials [45–47], semiconductors/superconductors [48], liquid crystals [49], ferroelectrics [50, 51], and high-harmonic generation in optical media [52].

Usually, hopfion states emerge in multicomponent systems or as quasi-linear modes confined by toroidal potentials. On the other hand, it was predicted that hopfions can be stabilized in inhomogeneous media with the repulsive nonlinearity even without a linear potential, provided the nonlinearity strength grows fast enough from the center to the periphery [53]. Stable toroidal modes with s=1 and vorticities m=0,1 have been predicted in the latter model.

While LHY superfluids were theoretically predicted [38] and experimentally observed [39], their precise configuration and spatial structure remain poorly understood. The known stabilization mechanism for 3D vortex modes, with topological charges up to m=8, by means of the balanced LHY nonlinearity and trapping potential [54] suggests two critical questions: (i) Can 3D twisted toroidal vortex states exist in LHY superfluids? (ii) What characterizes their dynamical evolution? Through numerical analysis of binary BECs trapped in a harmonic-oscillator (HO) trapping potential, we systematically investigate the existence, stability, and evolution of hopfions of this type. The findings demonstrate that the LHY-dominated hopfions undergo chemical-potential-dependent ex-

pansion, while maintaining their topological integrity. We show that hopfions with s=1 and m values at least up to 4 and sufficiently large number of particles exhibit exceptional stability, keeping the initial configurations without any observable deformation for an arbitrarily long time.

The following presentation is organized as follows. The model, based on the effective 3D GPE with the LHY term, is formulated in Section 2. Systematic numerical results, which reveal stable hopfion families, are reported in Section 3. In the same section, we discuss conditions for the experimental implementation of the predicted hopfion states. The paper is concluded by Section 4.

### 2. The model

In the MF approximation, a two-component BEC at zero temperature is modeled by the energy functional [55]

$$E_{\rm MF} = \int \left[ \sum_{i} \left( \frac{\hbar^2 |\nabla \Psi_i|^2}{2m_i} + R_i'(r)n_i \right) + \frac{1}{2} \sum_{ij} g_{ij} n_i n_j \right] d\mathbf{r}, \tag{1}$$

where subscripts i=1,2 denote the two components,  $\Psi_i(\mathbf{r})=\sqrt{N_i}\psi_i(\mathbf{r})$  represents the wave function of condensates with atom numbers  $N_i$  and particle densities  $n_i(\mathbf{r}) \equiv |\Psi_i(\mathbf{r})|^2$ , and  $R_i'(r)$  are trapping potentials. The interatomic interactions are determined by the coupling constants  $g_{ij}=2\pi\hbar^2a_{ij}(m_i+m_j)/(m_im_j)$ , where  $a_{ij}$  are the s-wave scattering lengths for collisions between atoms belonging to components i and j. In the case of equal masses  $(m_1=m_2\equiv m)$  and identical HO trapping potentials  $[R_1'(\mathbf{r})=R_2'(\mathbf{r})\equiv R'(\mathbf{r})=m\omega_0^2r^2/2]$ , the MF energy functional simplifies to

$$E_{\rm MF} = \int \left[ \frac{\hbar^2 (|\nabla \Psi_1|^2 + |\nabla \Psi_2|^2)}{2m} + R'(r)(n_1 + n_2) \right] d\mathbf{r}$$

$$+ \int \left[ \frac{4\pi\hbar^2}{m} (a_{11}n_1^2 + a_{22}n_2^2 + a_{12}n_1n_2) \right] d\mathbf{r}.$$
(2)

The intra-species stability of the model based on Eq. (2) is secured by positive intraspecies scattering lengths, i.e.,  $a_{11} > 0$ ,  $a_{22} > 0$ . When the inter-species negative (attractive) scattering length reaches the critical value  $a_{12} = -\sqrt{a_{11}a_{22}}$ , one eigenvalue of the quadratic form in Eq. (2) is zero and the other is positive. The eigenvector corresponding to the zero eigenvalue has  $n_2 = \sqrt{a_{11}/a_{22}}n_1$ . Therefore, the respective MF energy vanishes at this value of the density ratio, any deviation from it being energetically costly. More specifically, when both conditions  $a_{12} = -\sqrt{a_{11}a_{22}}$  and  $N_2/N_1 = \sqrt{a_{11}/a_{22}}$  are simultaneously satisfied, the MF terms are completely canceled in Eq. (2), and the corresponding strongly correlated condensate wavefunctions obey the constraint

$$\Psi_2 = \Psi_1 (a_{11}/a_{22})^{1/4}. \tag{3}$$

In this case, the MF interaction vanishes, and any perturbation to one component leads to a restoring force towards relation (3).

If the relatively strong MF interaction is canceled, the residual dynamics is dominated by the weak repulsive LHY nonlinearity. The LHY contribution to the energy density of the Bose mixture with equal masses m is [15]

$$\frac{\varepsilon_{\text{LHY}}}{V} = \frac{32\sqrt{2\pi}\hbar^2}{15m} \sum_{\pm} (a_{11}n_1 + a_{22}n_2 \pm \kappa)^{5/2}, \qquad (4)$$

with  $\kappa \equiv [(a_{11}n_1 - a_{22}n_2)^2 + 4a_{12}n_1n_2]^{1/2}$ . Under the conditions  $a_{12} = -\sqrt{a_{11}a_{22}}$  and  $n_1/n_2 = \sqrt{a_{22}/a_{11}}$ , the energy density is reduced to

$$\frac{\varepsilon_{\text{LHY}}}{V} = \frac{256\sqrt{\pi}\hbar^2}{15m} (n|a_{12}|)^{5/2}, \qquad (5)$$

where  $n = n_1 + n_2 \equiv |\Psi_1(\mathbf{r})|^2 + |\Psi_2(\mathbf{r})|^2$  is the total condensate density. Adding the above LHY correction to Eq. (2) and defining  $|\Psi|^2 \equiv |\Psi_1|^2 + |\Psi_2|^2$ , with  $\Psi_2 = \Psi_1(a_{11}/a_{22})^{1/4}$ , one obtains the effectively single-component energy functional

$$E = \int \left[ \frac{\hbar^2 |\nabla \Psi|^2}{2m} + R'(r) |\Psi|^2 + \frac{256 \sqrt{\pi} \hbar^2}{15m} |a_{12}|^{5/2} |\Psi|^5 \right] d\mathbf{r}.$$
 (6)

The corresponding GPE, with the nonlinearity stemming solely from the LHY terms, is derived in the following form:

$$i\hbar\frac{\partial\Psi}{\partial t} = \left[ -\frac{\hbar^2}{2m}\nabla^2 + R'(\mathbf{r}) + \frac{128\sqrt{\pi}\hbar^2}{3m} |a_{12}|^{5/2} |\Psi|^3 \right] \Psi. \tag{7}$$

Equation (7) is the model of the LHY superfluid in an interval around the value of the magnetic field which imposes the necessary Feshbach resonance [38]. To cast the GPE in the scaled form, we define characteristic units of length  $r_0 = \hbar/\sqrt{m\varepsilon_0}$ , time  $t_0 = \hbar/\varepsilon_0 = mr_0^2/\hbar$ . The characteristic factors for the normalization of the external potential and wave function are  $R = R'/\varepsilon_0$  and  $\psi = \Psi/\Psi_0$  with  $\Psi_0 = [3/(128\sqrt{\pi}r_0^2|a_{12}|^{5/2})]^{1/3}$ , respectively.

The so derived dimensionless GPE can be written as

$$i\frac{\partial \psi}{\partial t} = \left[ -\frac{1}{2} \nabla^2 + R(r) + |\psi|^3 \right] \psi. \tag{8}$$

It conserves norm N, energy E, and the angular momentum (in the case of spherically-symmetric potential), whose z-component  $M_z$  is written below:

$$N = \iiint |\psi|^2 d\mathbf{r},$$

$$E = \frac{1}{2} \iiint \left[ |\nabla \psi|^2 + \frac{4}{5} |\psi|^5 + 2R|\psi|^2 \right] d\mathbf{r},$$

$$M_z = i \iiint \left[ \psi^* \left( y \frac{\partial}{\partial x} - x \frac{\partial}{\partial y} \right) \psi \right] d\mathbf{r}$$
(9)

Stationary solutions for hopfions in the LHY superfluid can be defined, in cylindrical coordinates  $(\rho, \theta, z)$ , as

$$\psi(\mathbf{r}, t) = \phi(\rho, z) \exp(im\theta) \exp(-i\mu t), \tag{10}$$

where  $\mu$  is the chemical potential and  $m = \iint \arctan[\phi_i(x, y, z = 0)/\phi_r(x, y, z = 0)]dxdy/2\pi$  is the vorticity (topological charge)

of the vertical vortex line, where  $\phi_r$  and  $\phi_i$  are real and imaginary parts of the complex function  $\phi$ . Substituting ansatz (10) and considering the isotropic HO potential,  $R(\mathbf{r}) = \frac{1}{2}\omega^2(\rho^2 + z^2)$ , in Eq. (8) yields the stationary equation,

$$\frac{1}{2}\left(\frac{\partial^2}{\partial\rho^2}+\frac{1}{\rho}\frac{\partial}{\partial\rho}-\frac{m^2}{\rho^2}\right)\phi-\frac{1}{2}\omega^2(\rho^2+z^2)\phi+\mu\phi-|\phi|^3\phi=0. \eqno(11)$$

Solutions of Eq. (11) for the 3D LHY superfluid can be found by means of the Newton-conjugate-gradient [56] or relaxation method [57]. Below, we fix  $\omega = 0.1$  as a typical relevant value.

In contrast to the conventional vortex, with the single vortex line oriented parallel to the z-axis and described by real function  $\phi$  in Eq. (10), hopfions are represented by complex  $\phi \equiv \phi_r + i\phi_i$ , which has nontrivial phase structure due to the presence of the vortex ring,

$$\theta_s(x, z) = \arctan \frac{\phi_i(x, y = 0, z)}{\phi_r(x, y = 0, z)}.$$

The corresponding integer twist topological charge s is then found as

$$s = \frac{1}{2\pi} \iint \theta_s(x, z) \, \mathrm{d}x \mathrm{d}z.$$

## 3. Numerical results

Typical stationary solutions for twisted toroidal states with topological charges s = 1 and m = 0, 1, 2 are presented in Fig. 1. To the best of our knowledge, these states are the first reported examples of hopfions in the LHY superfluid. The vortex rings nested in nearly spherically-shaped hopfions are evident in the figures. The 3D plots demonstrate that the hopfion is based on the toroidal twisted vortex ring coiled around the z-axis, which is embedded in the 3D fundamental (m = 0) or vortex  $(m \ge 1)$  mode. At s = 0, the hopfion reduces to the conventional fundamental or conventional vortex mode [54]. The topological phase structure of the twisted vortex ring is displayed in the third column of Fig. 1. At a fixed chemical potential  $\mu$ , the dark hole surrounding the z-axis expands with the increase of m. The right column shows clearly the topology of vortex line and the pronounced phase discontinuity between the regions of  $\rho > R$  and  $\rho < R$ , where R is the radius of vortex ring. The z-component of the angular momentum of these states is related to the norm as in conventional vortices, viz.,  $M_z = mN$ . No hopfion modes with s > 1 have been found, even for m = 0.

Families of the hopfions with s=1 and m=0,1,2 are represented, in Fig. 2(a), by the dependence of the norm N on the chemical potential  $\mu$ , which shows monotonous increase of N with the growth of  $\mu$ . At fixed  $\mu$ , the hopfions with smaller values of vorticity m possess (slightly) higher norms. The hopfions cease to exist below a cutoff value  $\mu_{\rm cut}$  of the chemical potential, where N vanishes, and they transform into linear modes of the spherical HO potential, which makes it possible to find  $\mu_{\rm cut} = (m+s+3/2)\omega$ , as eigenvalues of the 3D HO potential.

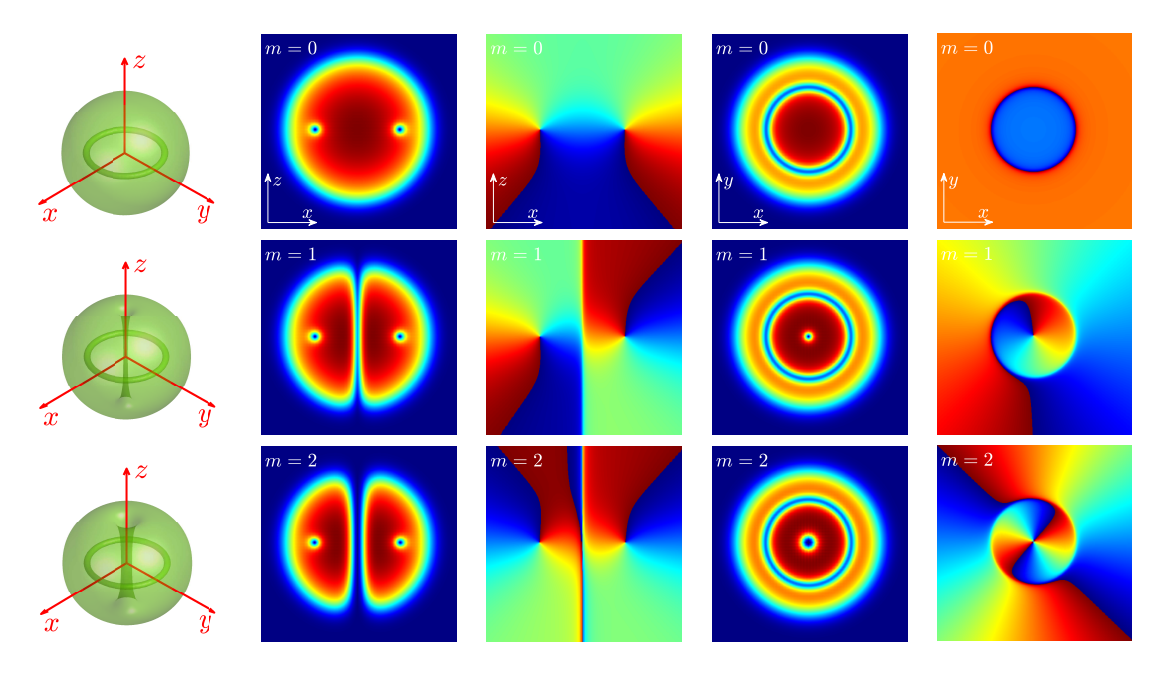


Fig. 1. (a) Top, central, and bottom rows: The hopfions with chemical potential  $\mu = 1.2$ , intrinsic winding number s = 1, and vorticities m = 0, 1, 2, maintained by the HO potential with  $\omega = 0.1$ . The first column shows the isosurface of  $|\phi(x, y, z)| = 0.45|\phi_{\text{max}}|$ . The second and third columns display  $|\phi|$  and  $\arg(\phi)$  in the cross section y = 0. The fourth and fifth columns show  $|\phi|$  and  $\arg(\phi)$  in the cross section z = 0. The spatial domain in all the 2D plots is [-20, +20]. Here and in other 2D figures, blue and red regions in plots of  $|\phi|$  correspond to lower and higher values, respectively.

The size of the hopfion is characterized by its effective width, defined by

$$W^2 \equiv \frac{\iiint (x^2 + y^2 + z^2)|\phi|^2 \mathrm{d}x \mathrm{d}y \mathrm{d}z}{N}.$$
 (12)

It exhibits a monotonic increase with the increase of N, indicating spatial expansion of the hopfions in condensates with larger atomic populations [Fig. 2(b)]. The hopfions with different values of m demonstrate nearly identical effective widths for fixed N, as shown in the inset of Fig. 2(b), where the hopfions with higher vorticity m exhibit a negligibly small increase of W in comparison with lower values of m. To enhance visual clarity in the main panel, we vertically offset the curves for m = 0 and m = 2 downward and upward by  $\Delta W = 1$ , respectively.

Figure 2(c) shows that the radius of the vortex ring increases with norm N, in contrast with the hopfions maintained by inhomogeneous self-repulsive media [53], where the radius of the coiled vortex thread slowly decreases with N, remaining finite (non-collapsing) as  $N \to \infty$ . The hopfions' amplitude also displays monotonous dependence on  $\mu$  for different values of m. This means that the maximum density of the atomic cloud increases with the growth of  $\mu$ .

The stability of the hopfions is the critically significant issue, as it determines their experimental observability of the modes. To explore the stability, we consider perturbed modes, looked for as

$$\psi(\rho, \theta, z, t) = [\phi(\rho, z) + f(\rho, z) \exp(\delta t + ik\theta) + g^*(\rho, z) \exp(\delta^* t - ik\theta)] \exp(-i\mu t + im\theta),$$

where f and g are the infinitesimal perturbations with the (generally, complex) growth rate  $\delta$ , the stability condition being that all eigenvalues must have  $\text{Re}(\delta) \leq 0$ , while k is an integer representing the angular index of the perturbations, and the asterisk stands for the complex conjugate. The substitution of the perturbed solutions in Eq. (8) leads to the linearized Bogoliubov – de Gennes equations [26], for the perturbations  $f(\rho, z)$  and  $g(\rho, z)$ :

$$i\delta f = -\frac{1}{2} \left( \frac{\partial^2}{\partial \rho^2} + \frac{1}{\rho} \frac{\partial}{\partial \rho} + \frac{\partial^2}{\partial z^2} - \frac{(k+m)^2}{\rho^2} \right) f$$

$$+ \left( \frac{5}{2} |\phi|^3 + V - \mu \right) f + \frac{3}{2} |\phi| \phi^2 g,$$

$$i\delta g = \frac{1}{2} \left( \frac{\partial^2}{\partial \rho^2} + \frac{1}{\rho} \frac{\partial}{\partial \rho} + \frac{\partial^2}{\partial z^2} - \frac{(k-m)^2}{\rho^2} \right) g$$

$$- \left( \frac{5}{2} |\phi|^3 + V - \mu \right) g - \frac{3}{2} |\phi| (\phi^*)^2 f.$$
(13)

Equations (13) can be solved by means of the Fourier collocation method [56].

The numerical solution of Eqs. (13) produces the stability regions for the hopfions with s=1 and m=0,1,2, according to Fig. 3, where the instability characteristics exhibit strong dependence of the azimuthal index k of the perturbations. Each value k=0,1,2 produces drastically different dependences of  $\text{Re}(\delta)$  on the hopfions's chemical potential  $\mu$ . The global instability domain is obtained of all particular ones corresponding to different values of k. For the hopfions with m=1 and 2, the instability spectrum is entirely dominated by the perturbations

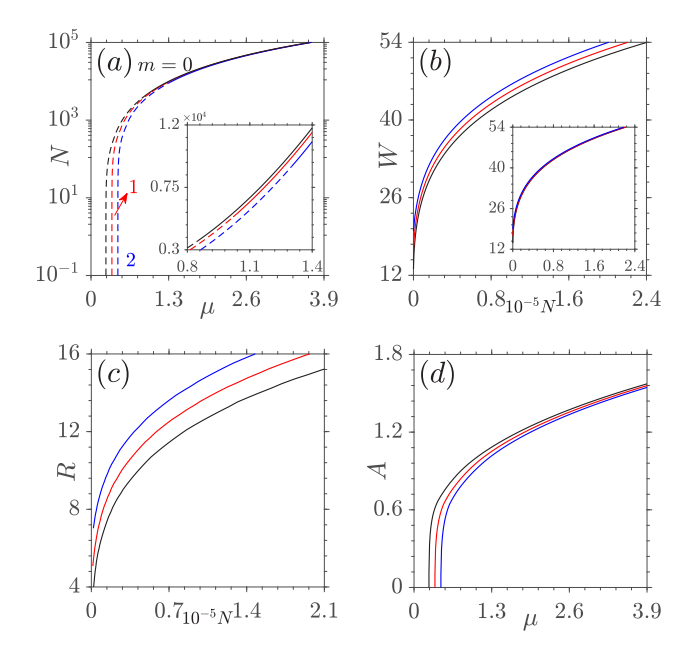


Fig. 2. Families of the twisted toroidal states (hopfions) with intrinsic winding number s=1 and different values of vorticity m: (a) the norm vs. the chemical potential; (b) the effective width vs. the norm; (c) radius R of the coiled vortex ring vs. the norm. (d) The dependence of the hopfion's amplitude,  $A=\max(|\phi|)$ , on  $\mu$ . The inset in (a) is the zoom-in, taken close to the border points separating stable (solid) and unstable (dashed) subfamilies. For the clarity's sake, the curves with m=0 and 2 (black and blues ones, respectively) in (b, c) are shifted by  $\Delta W(\Delta R) = -1$  and +1, respectively.

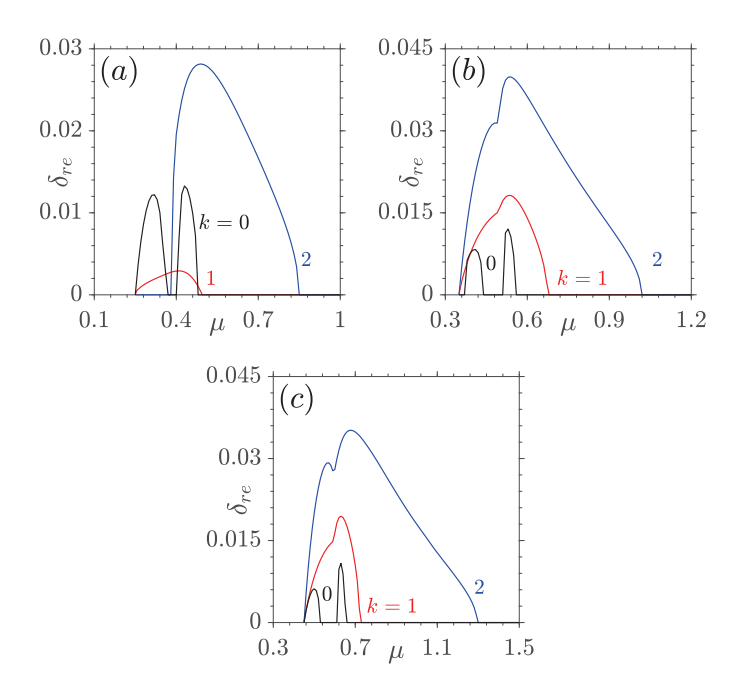


Fig. 3. The real part of the instability growth rate, for different values of azimuthal perturbation index k, versus the chemical potential. The instability domains are  $\mu \in [0.25, 0.85]$  for m = 0 (a), [0.35, 1.02] for m = 1 (b) and [0.45, 1.30] for m = 2 (c).

with k=2 [Figs. 3(b,c)], while the hopfions with m=0 show the dominant instabilities with k=0 and 1 at low norms, in addition to the leading instability with k=2 at larger norms [Fig. 3(a)]. The overall instability intervals are  $\mu \in [0.25, 0.85]$ , [0.35, 1.02], and [0.45, 1.3] for the hopfions with m=0, 1, and 2, respectively. Actually, the instability growth rates  $\text{Re}(\delta) > 0$  are small for unstable modes, which implies slow evolution of unstable hopfions, as shown below in Fig. 5.

In contrast to the fundamental state (s=0, m=0), which is completely stable in its existence domain [54], the hopfions with s=1 exhibit instability at low norms even for m=0. Nevertheless, the hopfions with different vorticities m achieve stabilization when their norm exceeds a threshold value, which is indicated by the solid-dashed-segment transitions in Fig. 2(a). The stability properties of the hopfions in the 3D LHY superfluid are in sharp contrast to those in the previously studied inhomogeneous repulsive media, where the hopfions with s=1, m=0 and s=1, m>1 are, respectively, completely stable and unstable in their entire existence domains [53].

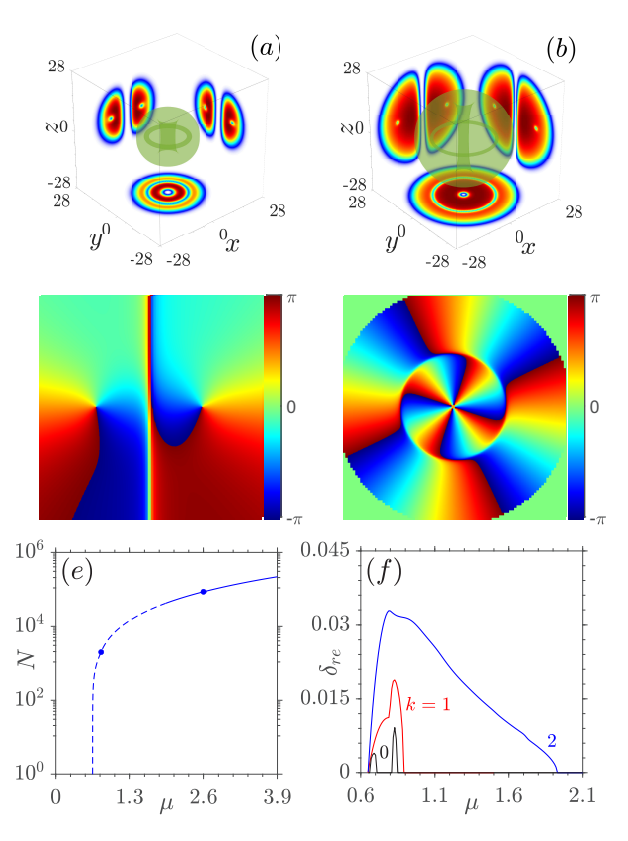


Fig. 4. Isosurfaces  $|\phi(x,y,z)| = 0.55\phi_{\text{max}}$  illustrating profiles of the hopfions with m=4, s=1 at  $\mu=1.1$  (a) and 2.6 (b). The 2D profiles on the walls and bottoms of the 3D boxes in (a) and (b) show the wave function in cross sections x=0, y=0, and z=0, respectively. (c, d) Phase distributions of  $\phi$  in cross sections y=0 and z=0. The spatial domains are  $(x,z) \in [-28, +28]$  in (c), and  $(x,y) \in [-28, +28]$  in (d). (e) Norm N vs. chemical potential  $\mu$  for the hopfions with m=4, s=1. (f) The instability growth rates vs.  $\mu$  for different values of azimuthal perturbation index k.

Further, we systematically investigated the hopfions with higher vorticities m. Representative examples of such solutions with s=1, m=4 are presented in Fig. 4. The hopfions exhibit characteristic features of twisted toroidal modes [Figs. 4(a,b)]. The phase structure in the (x,z) plane is typical for hopfions, where one can identify the presence of the vortex line and ring [Fig. 4(c)]. In the (x,y) plane, the vortex toroidal ring creates a pronounced phase discontinuity between the regions of  $\sqrt{x^2 + y^2} \equiv \rho > R$  and  $\rho < R$ , with R denoting the radius of the coiled vortex ring [Fig. 4(d)].

The hopfions with m=4 achieve the stability at  $N>N_{\rm cr}\approx 4\times 10^5$ . The perturbations with azimuthal index k=2 still dominate the instability in this case, the corresponding instability region being  $\mu\in[0.65,1.93]$ . While the theoretical results demonstrate that the hopfions with m>4 may be stabilized at even higher norms, the experimental realization of this prediction may face challenges due to the difficulty in preparing condensates with so large atom numbers.

To confirm the above predictions of the linear-stability analysis, we have conducted extensive simulations of the evolution of perturbed hopfions by dint of the split-step Fourier method. The results for stable hopfions are presented with white noise added to the input at t = 0. Representative examples are shown in Fig. 5. At  $\mu = 0.6$ , the vortex ring of the unstable hopfion with s = 1, m = 0 exhibits obvious deformation at t = 250, and is destroyed at t = 300 (the first row of Fig. 5). The corresponding maximum instability growth rate is 0.024 [Fig. 3(a)] is relatively small, thus allowing nearly stable evolution at t < 200. We note the instability develops even if noise is not initially added. On the other hand, the stable hopfion with s = 1, m = 2keeps its vortex line and ring intact in the course of an arbitrary long evolution (the second row of Fig. 5). The simulation results also show good agreement with the prediction of the linear-stability analysis for the hopfions with higher values of vorticity m. For instance, the maximal instability growth rate of the hopfion with m = 4 at  $\mu = 1.5$  is 0.0125, see Fig. 4(f). This small value expectedly delays the onset of the deformation of the vortex ring. A perturbed stable hopfion with larger norm quickly radiates away the initially added noise and then keeps its robust structure in the course of indefinitely long evolution (see the fourth row of Fig. 5). It is worthy to note that stable hopfions with  $m \ge 2$  in single-component models have not been previously reported.

Finally, we note that the experimental realization of the predicted hopfions can be achieved using the setup proposed in Ref. [39]. In this context, we consider the <sup>39</sup>K atomic gas, which was used in recent experimental configurations [22, 24, 39]. Setting  $r_0 = 0.3 \, \mu \text{m}$  yields a characteristic time scale  $t_0 \sim 55.2 \, \text{ms}$ . The scattering lengths are chosen as  $|a_{12}| = \sqrt{a_{11}a_{22}} = 53a_0$  with  $a_{22}/a_{11} = 2.5$  ( $a_0$  is the Bohr radius). The frequency of HO potential is  $\omega = \omega_0 r_0 \, \sqrt{m/\varepsilon_0}$ , where  $\omega_0$  represents the actual trapping frequency. The physical atom number N relates to the dimensionless norm N through  $N = (\varepsilon_0 r_0^3/g_{12})N$  with the coupling constant  $g_{12} = 4\pi \hbar^2 a_{12}/m$ . Based on these parameters, we estimate feasible values for the proposed experimental realization as  $\omega_0 \sim 288.13 \times 2\pi \, \text{Hz}$ , and  $N \sim 4.26 \times 10^4$ , all being within the range of current experi-

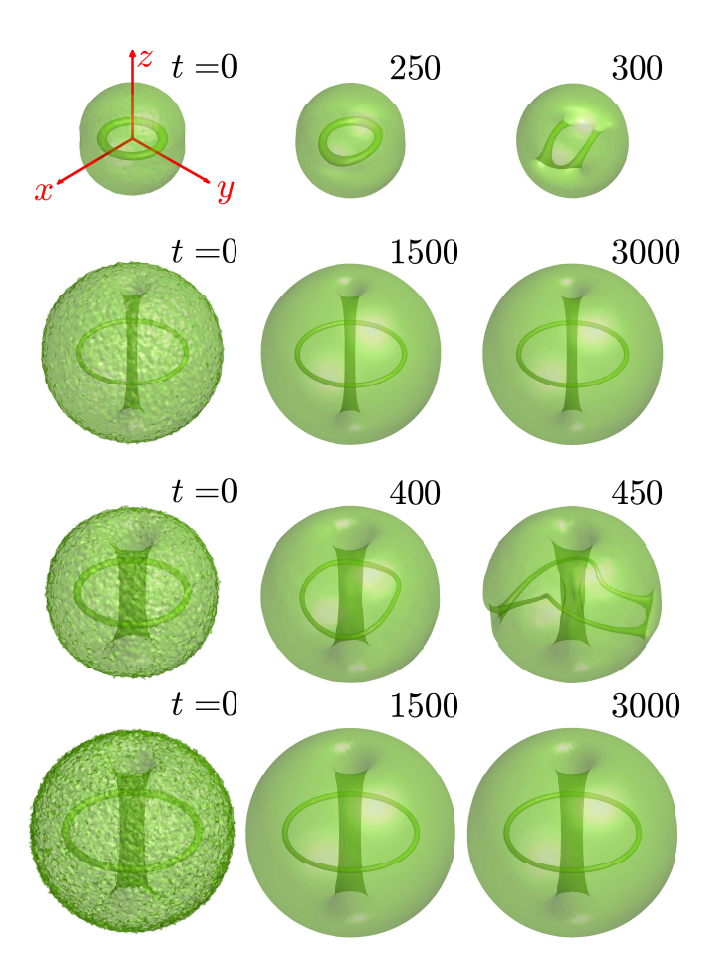


Fig. 5. Isosurfaces  $|\phi(x, y, z)| = 0.35 |\phi|_{\text{max}}$  and  $0.45 |\phi|_{\text{max}}$  in the first three rows, and in the bottom one, show, respectively, the unstable evolution of the hopfions with  $m = 0, \mu = 0.6$  and  $m = 4, \mu = 1.5$  (the first and third rows, respectively), and the stable evolution for  $m = 2, \mu = 1.5$  and  $m = 4, \mu = 2.16$  (the second and fourth rows). Broadband random perturbations are applied to all hopfions at t = 0. In all cases, the twist topological charge is s = 1.

mental capabilities.

### 4. Conclusion

In this work we have investigated the stationary states and dynamics of the 3D LHY (Lee-Huang-Yang) superfluid in the regime where the MF (mean-field) interactions are completely canceled, the LHY nonlinearity being the dominant term. The system is modeled by the effective single-component GPE (Gross-Pitaevskii equation), featuring zero inter-component interaction and quartic LHY self-repulsion. Hopfions, as 3D complex topological states, can be created in the corresponding binary BEC if the self-repulsion is balanced by the HO (harmonic-oscillator) potential. These hopfions exhibit coexisting vortex line and vortex ring, characterized by two independent topological winding numbers: overall vorticity m and twist s. We have identified families of stable hopfions with s=1 and

m ranging from 0 to 4. The norm, effective radius, peak density, and radius of coiled vortex ring all increase with the growth of the hopfion's chemical potential. Although the instability domain of the hopfions expands with the increase of m, such stable states have been found in a wide parameter region (at least, for  $m \le 4$ ), provided that the norm exceeds a threshold value.

**CRediT authorship contribution statement** Liangwei Dong: Conceptualization and writing the original draft; Mingjing Fan: Numerical calculations; Boris A. Malomed: Analytical investigation and work on the draft; Yaroslav V. Kartashov: Review, editing and validation.

**Declaration of competing interest** The authors declare that they have no known competing financial interests or personal relationships that could have appeared to influence the work reported in this paper.

Data availability Data will be made available on request.

**Acknowledgments** This work is supported by the Natural Science Basic Research Program of Shaanxi Province of China (Grant No. 2022JZ-02) and Israel Science Foundation (Grant No. 1695/22). Y.V.K. acknowledges funding by the research project FFUU-2024-0003 of the Institute of Spectroscopy of the Russian Academy of Sciences.

### References

- Y. V. Kartashov, B. A. Malomed, L. Torner, Solitons in nonlinear lattices, Rev. Mod. Phys. 83 (2011) 247–305.
- [2] B. A. Malomed, Multidimensional Solitons, AIP Publishing LLC, 2022.
- [3] I. Shomroni, E. Lahoud, S. Levy, J. Steinhauer, Evidence for an oscillating soliton/vortex ring by density engineering of a Bose-Einstein condensate, Rev. Mod. Phys. 5 (2009) 193–197.
- [4] Y. Zhao, Q. Huang, T. Gong, S. Xu, Z. Li, B. A. Malomed, Three-dimensional solitons supported by the spin-orbit coupling and Rydberg-Rydberg interactions in PT-symmetric potentials, Chaos Solitons Fractals 187 (2024) 115329.
- [5] N. R. Cooper, Propagating Magnetic Vortex Rings in Ferromagnets, Phys. Rev. Lett. 82 (1999) 1554–1557.
- [6] J. Junquera, Y. Nahas, S. Prokhorenko, L. Bellaiche, J. Iniguez, D. G. Schlom, L.-Q. Chen, S. Salahuddin, D. A. Muller, L. W. Martin, R. Ramesh, Topological phases in polar oxide nanostructures, Rev. Mod. Phys. 95 (2023) 025001.
- [7] E. Radu, M. S. Volkov, Stationary ring solitons in field theory-Knots and vortons, Phys. Rep. 468 (4) (2008) 101–151.
- [8] P. M. Saffin, Q.-X. Xie, S.-Y. Zhou, Q-Ball Superradiance, Phys. Rev. Lett. 131 (2023) 111601.
- [9] L. Bergé, Wave collapse in physics: principles and applications to light and plasma waves, Phys. Rep. 303 (5) (1998) 259–370.
- [10] V. E. Zakharov, E. A. Kuznetsov, Solitons and collapses: two evolution scenarios of nonlinear wave systems, Phys. Usp. 55 (6) (2012) 535–556.
- [11] G. Fibich, The Nonlinear Schrödinger Equation: Singular solutions and optical collapse, in: The Nonlinear Schrödinger Equation, vol. 192, Springer Heidelberg, 2015.
- [12] Y. S. Kivshar, G. P. Agrawal, Optical solitons: from fibers to photonic crystals, Academic Press, San Diego, 2003.
- [13] L. Pitaevskii, S. Stringari, Bose-Einstein Condensation, Oxford University Press, Oxford, 2003.
- [14] T. D. Lee, K. Huang, C. N. Yang, Eigenvalues and Eigenfunctions of a Bose System of Hard Spheres and Its Low-Temperature Properties, Phys. Rev. 106 (1957) 1135–1145.
- [15] D. S. Petrov, Quantum Mechanical Stabilization of a Collapsing Bose-Bose Mixture, Phys. Rev. Lett. 115 (2015) 155302.
- [16] D. S. Petrov, G. E. Astrakharchik, Ultradilute Low-Dimensional Liquids, Phys. Rev. Lett. 117 (2016) 100401.

- [17] D. Jaksch, C. Bruder, J. I. Cirac, C. W. Gardiner, P. Zoller, Cold Bosonic Atoms in Optical Lattices, Phys. Rev. Lett. 81 (1998) 3108–3111.
- [18] B. Yang, H. Sun, C.-J. Huang, H.-Y. Wang, Y. Deng, H.-N. Dai, Z.-S. Yuan, J.-W. Pan, Cooling and entangling ultracold atoms in optical lattices, Science 369 (2020) 550–553.
- [19] M. Greiner, O. Mandel, T. Esslinger, T. W. Hänsch, I. Bloch, Quantum phase transition from a superfluid to a Mott insulator in a gas of ultracold atoms, Nature 415 (2002) 39–44.
- [20] X. Zhang, C.-L. Hung, S.-K. Tung, C. Chin, Observation of quantum criticality with ultracold atoms in optical lattices, Science 335 (2012) 1070–1072.
- [21] H. Kadau, M. Schmitt, M. Wenzel, C. Wink, T. Maier, I. Ferrier-Barbut, T. Pfau, Observing the Rosensweig instability of a quantum ferrofluid, Nature 530 (2016) 194.
- [22] C. R. Cabrera, L. Tanzi, J. Sanz, N. Naylor, P. Thomas, P. Cheiney, T. L., Quantum liquid droplets in a mixture of Bose-Einstein condensates, Science 359 (2018) 301.
- [23] P. Cheiney, C. R. Cabrera, J. Sanz, B. Naylor, L. Tanzi, L. Tarruell, Bright Soliton to Quantum Droplet Transition in a Mixture of Bose-Einstein Condensates, Phys. Rev. Lett. 120 (2018) 135301.
- [24] G. Semeghini, G. Ferioli, L. Masi, C. Mazzinghi, L. Wolswijk, F. Minardi, M. Modugno, G. Modugno, M. Inguscio, M. Fattori, Self-Bound Quantum Droplets of Atomic Mixtures in Free Space, Phys. Rev. Lett. 120 (2018) 235301.
- [25] I. Ferrier-Barbut, T. Pfau, Quantum liquids get thin, Science 359 (2018) 274
- [26] Y. V. Kartashov, B. A. Malomed, L. Tarruell, L. Torner, Threedimensional droplets of swirling superfluids, Phys. Rev. A 98 (2018) 013612.
- [27] Y. Li, Z. Chen, Z. Luo, C. Huang, H. Tan, W. Pang, B. A. Malomed, Twodimensional vortex quantum droplets, Phys. Rev. A 98 (2018) 063602.
- [28] X. Zhang, X. Xu, Y. Zheng, Z. Chen, B. Liu, C. Huang, B. A. Malomed, and Y. Li, Semidiscrete quantum droplets and vortices, Phys. Rev. Lett. 123 (2019) 133901.
- [29] M. Tylutki, G. E. Astrakharchik, B. A. Malomed, D. S. Petrov, Collective excitations of a one-dimensional quantum droplet, Phys. Rev. A 101 (2020) 051601(R).
- [30] L. Dong, Y. V. Kartashov, Rotating Multidimensional Quantum Droplets, Phys. Rev. Lett. 126 (2021) 244101.
- [31] I. Ferrier-Barbut, H. Kadau, M. Schmitt, M. Wenzel, T. Pfau, Observation of Quantum Droplets in a Strongly Dipolar Bose Gas, Phys. Rev. Lett. 116 (2016) 215301.
- [32] M. Schmitt, M. Wenzel, F. Böttcher, I. Ferrier-Barbut, T. Pfau, Self-bound droplets of a dilute magnetic quantum liquid, Nature 539 (2016) 259.
- [33] G. Ferioli, G. Semeghini, S. Terradas-Brianso, L. Masi, M. Fattori, M. Modugno, Dynamical formation of quantum droplets in a <sup>39</sup>K mixture, Phys. Rev. Res. 2 (2020) 013269.
- [34] C. D'Errico, A. Burchianti, M. Prevedelli, L. Salasnich, F. Ancilotto, M. Modugno, F. Minardi, C. Fort, Observation of quantum droplets in a heteronuclear bosonic mixture, Phys. Rev. Res. 1 (2019) 033155.
- [35] R. N. Bisset, L. A. P. n. Ardila, L. Santos, Quantum Droplets of Dipolar Mixtures, Phys. Rev. Lett. 126 (2021) 025301.
- [36] J. C. Smith, D. Baillie, P. B. Blakie, Quantum Droplet States of a Binary Magnetic Gas, Phys. Rev. Lett. 126 (2021) 025302.
- [37] C. Fort, M. Modugno, Self-Evaporation Dynamics of Quantum Droplets in a <sup>41</sup>K-<sup>87</sup>Rb Mixture, Appl. Sci. 1 (2021) 866.
- [38] N. B. Jørgensen, G. M. Bruun, J. J. Arlt, Dilute Fluid Governed by Quantum Fluctuations, Phys. Rev. Lett. 121 (2018) 173403.
- [39] T. G. Skov, M. G. Skou, N. B. Jørgensen, J. J. Arlt, Observation of a Lee-Huang-Yang Fluid, Phys. Rev. Lett. 126 (2021) 230404.
- [40] X. Liu, J. Zeng, One-dimensional purely Lee-Huang-Yang fluids dominated by quantum fluctuations in two-component Bose-Einstein condensates, Chaos Soliton Fract. 160 (2022) 112240.
- [41] H. Hopf, Über die Abbildungen der dreidimensionalen Sphäre auf die Kugelfläche, Math. Ann 104 (1931) 637–665.
- [42] C. Wan, Y. Shen, A. Chong, Q. Zhan, Scalar optical hopfions, eLight 2 (2022) 22.
- [43] L. D. Faddeev, A. J. Niemi, Knots and particles, Nature 387 (1997) 58-61.
- [44] N. Manton, P. Sutcliffe, Topological Solitons (Cambridge University Press, Cambridge, 2004).
- [45] B. Göbel, I. Mertig, O. A. Tretiakov, Beyond skyrmions: Review and

- perspectives of alternative magnetic quasiparticles, Phys. Rep. 895 (2021) 1,28
- [46] F. N. Rybakov, N. S. Kiselev, A. B. Borisov, L. Doering, C. Melcher, S. Bluegel, Magnetic hopfions in solids, APL Materials 10 (2022) 1814338.
- [47] F. Zheng, N. S. Kiselev, F. N. Rybakov, L. Yang, W. Shi, S. Blügel, R. E. Dunin-Borkowski, Hopfion rings in a cubic chiral magnet, Nature 623 (2023) 718–723.
- [48] E. Babaev, Non-Meissner electrodynamics and knotted solitons in twocomponent superconductors, Phys. Rev. B 79 (2009) 104506.
- [49] P. J. Ackerman, I. I. Smalyukh, Diversity of knot solitons in liquid crystals manifested by linking of preimages in torons and hopfions, Phys. Rev. X 7 (2017) 011006.
- [50] I. Lukyanchuk, Y. Tikhonov, A. Razumnaya, V. Vinokur, Hopfions emerge in ferroelectrics, Nat. Commun. 11 (2020) 2433.
- [51] I. Lukyanchuk, A. Razumnaya, S. Kondovych, Y. Tikhonov, B. Khesin, V. Vinokur, Topological foundations of ferroelectricity, Phys. Rep. 1110 (2025) 1–56.
- [52] Z. Lyu, Y. Fang, Y. Liu, Formation and Controlling of Optical Hopfions in High Harmonic Generation, Phys. Rev. Lett. 133 (2024) 133801.
- [53] Y. V. Kartashov, B. A. Malomed, Y. Shnir, L. Torner, Twisted Toroidal Vortex Solitons in Inhomogeneous Media with Repulsive Nonlinearity, Phys. Rev. Lett. 113 (2014) 264101.
- [54] L. Dong, M. Fan, Stable higher-charge vortex droplets governed by quantum fluctuations in three dimensions, Chaos Solitons Fractals 173 (2023) 113728.
- [55] C. J. Pethick, H. Smith, Bose–Einstein condensation in dilute gases, Cambridge university press, 2008.
- [56] J. Yang, Nonlinear Waves in Integrable and Nonintegrable Systems, SIAM, Philadelphia, 2010.
- [57] C. Besse, A Relaxation Scheme for the Nonlinear Schrödinger Equation, SIAM Journal on Numerical Analysis 42 (2004) 934–952.